Editors' Suggestion

Coupled Bogoliubov equations for electrons and phonons

C.-Yu Wang [1,2] S. Sharma [3] T. Müller,[1] E. K. U. Gross,[2] and J. K. Dewhurst [1,*]

[1]*Max-Planck-Institut für Mikrostrukturphysik, Weinberg 2, D-06120 Halle, Germany*

[2]*Fritz Haber Center for Molecular Dynamics, Institute of Chemistry, The Hebrew University of Jerusalem, Jerusalem 91904, Israel*

[3]*Max-Born-Institute for Non-linear Optics and Short Pulse Spectroscopy, Max-Born Strasse 2A, 12489 Berlin, Germany*

(Received 18 January 2022; revised 7 April 2022; accepted 7 April 2022; published 16 May 2022)

With the aim of including small amplitude quantum nuclear dynamics in solid-state calculations, we derive a set of equations by applying Wick's theorem to the square of the Fröhlich Hamiltonian. These are noninteracting fermionic and bosonic Hamiltonians with terms up to quadratic order in the field operators. They depend on one another's density matrices and are therefore to be solved self-consistently. A Bogoliubov transformation is required to diagonalize both the fermionic and bosonic Hamiltonians since they represent noninteracting quantum field theories with an indefinite number of particles. The Bogoliubov transform for phonons is non-Hermitian in the general case, and the corresponding time evolution is nonunitary. Several sufficient conditions for ensuring that the bosonic eigenvalues are real are provided. The method was implemented in an all-electron code and shown to correctly predict the renormalization of the Kohn-Sham band gap of diamond and silicon due to the electron-phonon interaction. The theory also verifies that niobium and MgB_2 are phonon-mediated superconductors and predicts the existence and magnitude of their superconducting gaps. Lastly, we confirm that copper is *not* a superconductor even at zero temperature.

DOI: 10.1103/PhysRevB.105.174509

I. INTRODUCTION

The adiabatic approximation is among the most fundamental ingredients of modern condensed-matter theory and quantum chemistry. It rests on the intuitive picture that the electrons, being much lighter than the nuclei, can instantaneously adjust to the nuclear positions. A two-step approach of first evaluating the Born-Oppenheimer (BO) potential energy surface [1–4] with electronic-structure methods and then solving the nuclear Schrödinger equation in terms of vibrational degrees of freedom is a standard procedure in the *ab initio* treatment of molecules and solids. The adiabatic approximation is crucial here because it leads to separate equations for the electronic and nuclear degrees of freedom, respectively. It is this separation that allows us to treat the electronic and nuclear many-body problems with very different methodologies. The adiabatic approximation not only makes computations feasible, it is deeply ingrained in the way we visualize the atomic and electronic structure of molecules and solids.

Yet some of the most fascinating phenomena in condensed matter physics and quantum chemistry live outside the realm of the adiabatic approximation. Prime examples are phonon-mediated superconductivity [5] or the process of vision [6]. The theoretical treatment of nonadiabatic phenomena is notoriously difficult because one is basically forced to go back to the full electron-nuclear Schrödinger equation.

In molecules, nonadiabaticity is mainly associated with transitions between different BO potential energy surfaces: If a traveling nuclear wave packet reaches a conical intersection, i.e., a point where it is nearly or fully degenerate with another BO surface, then this can trigger the nuclear wave packet to split, leading to a significant population in both surfaces. Continuing its journey, the wave packet may split again when it encounters avoided crossings with other BO surfaces and, when returning, it may interfere with parts of itself. This rolling-around of nuclear amplitudes on BO surfaces is the essence of most photochemical and photophysical processes [7,8]. Sometimes the nuclear wave packet returns to where it started from, thus completing an optical cycle as found in the process of vision [6] or photosynthesis [9]. All these effects go along with large-amplitude nuclear motion which cannot easily be captured in terms of phonon modes. Here the natural strategy is to represent the nuclear wave packets in terms of classical trajectories in one way or another.

In solids, however, the nuclei tend to stay close to their equilibrium positions (unless the temperature gets close to the melting point). Nuclear motion is then well described in terms of phonon modes, and nonadiabaticity shows up as the electron-phonon interaction. Prime examples of nonadiabatic effects in this regime are phonon-mediated superconductivity [5], the renormalization of the band gap in insulators and semiconductors [10], as well as a phonon-induced modification of the electron dispersion in metals near the Fermi surface [11].

In the dynamics of strongly driven electrons and, likewise, in electron transport, electron-phonon scattering is an important damping mechanism. After exciting a metal with a strong laser pulse, the initial nonthermal distribution first reaches a purely electronic equilibrium within some tens of femtoseconds, and on the timescale of picoseconds, electron-phonon

*dewhurst@mpi-halle.mpg.de

scattering leads to a thermalization of the complete system of electronic and lattice degrees of freedom [12]. Similarly, magnon-phonon scattering is one of the mechanisms responsible for the damping of ultrafast spin-dynamics effects such as optical inter-site spin transfer [13]. In all these examples, dissipation, i.e., the transfer of energy from the electronic to the nuclear subsystem, is the relevant mechanism. Another important aspect is the influence of phonons on exciton dynamics. In some cases, the migration of excitons (which is essential for producing a photo-current in photovoltaic devices) is enabled through nonadiabatic electron-nuclear coupling, while for clamped nuclei the migration of excitons may be blocked [14–16].

The goal of this paper is to develop a single *ab initio* method able to predict all of the above nonadiabatic phenomena associated with small-amplitude nuclear motion in solids. The essence of our proposal is solve two coupled Bogoliubov equations alongside each other, one describing the electrons, the other treating the phononic degrees of freedom. Bogoliubov equations represent systems of noninteracting particles in terms of state vectors which are not eigenfunctions of the particle-number operator. This choice is deliberate and important. For the electronic subsystem, Bogliubov equations provide the natural framework to calculate the superconducting order parameter. Treating the phononic subsystem by a Bogoliubov equation as well is a less obvious choice but it is essential. Phonons can be generated from both the electron-phonon interaction (virtual phonons) or by an external influence such as a laser pulse (real phonons). Hence the number of phonons cannot be a conserved quantity. The two Bogoliubov equations are coupled through effective potentials which depend on the electronic and phononic normal and anomalous density matrices and on the electron-phonon coupling matrix. The two equations are solved self-consistently (in the stationary case) or propagated in time alongside each other. The influence goes both ways: The phonons, described by the bosonic Bogoliubov equation, renormalize the electronic band structure and/or make the system superconducting. Likewise, the electronic degrees of freedom renormalize the phonon spectrum, giving rise, for example, to a Kohn anomaly [17] or to modifications of the phonon spectrum due to the presence of superconductivity [18]. An important virtue of this method is that both real and virtual phonons arise from the same noninteracting state, which itself has been properly time evolved. This puts strong constraints on the phonon density matrices.

A necessary step in this paper is the construction of approximations for effective potentials as functionals of the normal and anomalous density matrices and the electron-phonon vertex,

$$\Gamma^{\alpha\mathbf{q}}_{ij\mathbf{k}} = \sum_{ap} \frac{\mathbf{e}^{\alpha\mathbf{q}}_{ap}}{\sqrt{2M_a\nu_{\alpha\mathbf{q}}}} \langle \varphi_{i\mathbf{k}+\mathbf{q}} | \partial \hat{V}_s / \partial u^{\mathbf{q}}_{ap} | \varphi_{j\mathbf{k}} \rangle, \tag{1}$$

where i and j label Kohn-Sham [19] orbitals with momentum $\mathbf{k}+\mathbf{q}$ and $\mathbf{k}$, respectively; $\hat{V}_s$ is the Kohn-Sham potential operator; $u^{\mathbf{q}}_{ap}$ is a displacement of atom a in Cartesian direction p with phase $e^{i\mathbf{q}\cdot\mathbf{r}}$; M_a is the mass of the atom; $\mathbf{e}^{\alpha\mathbf{q}}_{ap}$ is the eigenvector of phonon mode $(\alpha, \mathbf{q})$; and $\nu_{\alpha\mathbf{q}}$ is the phonon frequency. The construction makes use of the fact that, unlike the electron- only many-body problem, the coupled electron-nuclear system has a small parameter, the electron-nuclear mass ratio m/M, where m is the electron mass and M is a nuclear reference mass. In terms of this dimensionless parameter, the harmonic phonon frequencies are of order $(m/M)^{1/2}$. Anharmonic effects in the phonon frequencies show up in order $(m/M)^{3/4}$ and the lowest energy correction produced by the electron-phonon interaction is of order $(m/M)^{1/2}$. By virtue of Migdal's theorem, we know that the next order is smaller by another factor of $(m/M)^{1/2}$, and is therefore usually negligible. Our construction of the approximate functionals is based on the same principle: We consistently include all contributions to order $(m/M)^{1/2}$ and, in line with Migdal's theorem, neglect all higher-order contributions to the potentials.

In Sec. II, we describe how this is achieved in practice: The idea is to apply Wick's theorem to the square of the Fröhlich Hamiltonian [20]. This yields fermionic and bosonic Bogoliubov equations as well as explicit forms for their potentials. In Sec. III, we work out the algebraic structure of these Bogoliubov equations. Special attention will be given to the non-Hermitian nature of the bosonic Hamiltonian. The results of this section are quite general and apply equally to the equations describing the coupled motion of electrons and magnons, electrons and photons, or any other bosonic species coupled to the electronic system. In Sec. IV, we provide some details about the implementation for solids. Finally, in Sec. V, we will demonstrate the efficacy of the proposed method by computing the renormalized Kohn-Sham band gaps of diamond and silicon and also the superconducting gaps of niobium and MgB_2; as well as verifying that copper is *not* a superconductor at zero temperature. In doing so, we introduce two potential observables which provide detailed information on where in the reciprocal space electron-phonon interactions are the strongest. A major long-term aim of this paper is to perform a parameter-free, *ab initio* time evolution of the superconducting state for any solid. This would normally be prohibitively expensive with Green's function methods (although, see Karlsson *et al.* [21]). Time evolving the noninteracting bosonic state alongside the electronic state is, however, a practical method for such a simulation because all equations are first order in time and merely require a simple time-step integration. Such calculations would enable study of effects such as photoinduced superconductivity on short timescales by shaped laser pulses [22–25].

II. MEAN-FIELD THEORY OF A SQUARED HAMILTONIAN

Our aim is to replace an interacting Hamiltonian with a pair of noninteracting Hamiltonians, coupled only indirectly by their density matrices. In general, such Hamiltonians can be diagonalized using Bogoliubov transforms. Solutions to the Bogoliubov equations can then be used to obtain various observables needed for a unified description of the phenomena mention above such as band-gap renormalization and superconductivity.

We begin with a generalized Fröhlich Hamiltonian for solids,

$$\hat{H}_{\rm F} = \sum_{i\mathbf{k}} \epsilon_{i\mathbf{k}} \hat{a}^\dagger_{i\mathbf{k}} \hat{a}_{i\mathbf{k}} + \sum_{\alpha\mathbf{q}} \nu_{\alpha\mathbf{q}} \hat{d}^\dagger_{\alpha\mathbf{q}} \hat{d}_{\alpha\mathbf{q}} + \sum_{ij\mathbf{k},\alpha\mathbf{q}} \Gamma^{\alpha\mathbf{q}}_{ij\mathbf{k}} \hat{a}^\dagger_{i\mathbf{k}+\mathbf{q}} \hat{a}_{j\mathbf{k}} (\hat{d}_{\alpha\mathbf{q}} + \hat{d}^\dagger_{\alpha-\mathbf{q}}), \tag{2}$$

where $\epsilon_{i\mathbf{k}}$ is taken to be the ith eigenvalue of a noninteracting system (typically Kohn-Sham [19]) at k-point $\mathbf{k}$; $\nu_{\alpha\mathbf{q}}$ is the αth phonon frequency at q-point $\mathbf{q}$; and $\Gamma^{\alpha\mathbf{q}}_{ij\mathbf{k}}$ are the electron-phonon coupling matrix elements from Eq. (1).

The Hamiltonian in Eq. (2) contains an interaction term (i.e., beyond quadratic order in the operators) and thus cannot be solved exactly. Instead we employ Wick's theorem [26], which rewrites $\hat{H}_{\rm F}$ as a sum of normal-ordered products arranged from uncontracted terms to fully contracted products. Our approximation is then to keep all terms up to quadratic order. Applying this strategy directly to $\hat{H}_{\rm F}$ results in two problems. The first is that a nontrivial solution would require that $\langle \hat{d}_{\alpha\mathbf{q}} + \hat{d}^\dagger_{\alpha-\mathbf{q}} \rangle \neq 0$, which would imply that the atoms have displaced. However, the superconducting transition is not brought about by an atomic displacement. For example, a solid with one atom per unit cell, such as bcc niobium, cannot undergo an atomic displacement across the transition and remain lattice periodic. The second problem is that there is no anomalous term of the form $\langle \hat{a}^\dagger \hat{a}^\dagger \rangle$ in the Wick expansion of $\hat{H}_{\rm F}$. These issues preclude the use of this approximation for superconductivity calculations.

We now make the observation that any operator raised to a power has the same eigenvectors as the original. In particular, if $\hat{H}_{\rm F}|\Psi_i\rangle = E_i|\Psi_i\rangle$ then

$$\hat{H}^2_{\rm F}|\Psi_i\rangle = E_i^2|\Psi_i\rangle, \tag{3}$$

which can be used to determine the ground state of $\hat{H}_{\rm F}$ with the proviso that the sign of each E_i be determined independently. Wick's theorem applied to $\hat{H}^2_{\rm F}$ overcomes both aforementioned problems, namely that nontrivial solutions do not require atomic displacements and there is now an anomalous term in the Wick expansion.

The first term in the Wick expansion of $\hat{H}^2_{\rm F}$ is the direct term from the noninteracting part of the electronic Hamiltonian:

$$2\left[\frac{n_s}{N_k}\sum_{j\mathbf{k}'} \epsilon_{j\mathbf{k}'} \overbrace{\hat{a}^\dagger_{j\mathbf{k}'} \hat{a}}\,_{j\mathbf{k}'} + \frac{1}{N_q}\sum_{\alpha\mathbf{q}} \nu_{\alpha\mathbf{q}} \overbrace{\hat{d}^\dagger_{\alpha\mathbf{q}} \hat{d}}\,_{\alpha\mathbf{q}}\right] \sum_{i\mathbf{k}} \epsilon_{i\mathbf{k}} \hat{a}^\dagger_{i\mathbf{k}} \hat{a}_{i\mathbf{k}} = 2\,\delta E_0 \sum_{i\mathbf{k}} \epsilon_{i\mathbf{k}} \hat{a}^\dagger_{i\mathbf{k}} \hat{a}_{i\mathbf{k}}, \tag{4}$$

where $n_s = 1$ and $n_s = 2$ for spin-polarized and spin-unpolarized calculations, respectively, and the change in the noninteracting energy per unit cell is given by

$$\delta E_0 = \frac{n_s}{N_k}\sum_{i\mathbf{k}} \epsilon_{i\mathbf{k}}\, \delta\gamma^{\mathbf{k}}_{ij} + \frac{1}{N_q}\sum_{\alpha\mathbf{q}} \nu_{\alpha\mathbf{q}} \langle \hat{d}^\dagger_{\alpha\mathbf{q}} \hat{d}_{\alpha\mathbf{q}} \rangle. \tag{5}$$

Here the change in electronic density matrix is given by

$$\delta\gamma^{\mathbf{k}}_{ij} = \gamma^{\mathbf{k}}_{ij} - \Theta(\epsilon_{i\mathbf{k}} - \epsilon_{\rm F})\delta_{ij}, \tag{6}$$

with

$$\gamma^{\mathbf{k}}_{ij} = \langle \hat{a}^\dagger_{i\mathbf{k}} \hat{a}_{j\mathbf{k}} \rangle. \tag{7}$$

Taking $\overbrace{\hat{a}^\dagger_{i\mathbf{k}} \hat{a}}\,_{j\mathbf{k}}$ to mean the change in the density matrix in Eq. (6), rather than the density matrix itself, is equivalent to first placing the Hamiltonian in particle-hole form. A consequence of this is that $\delta E_0 \geqslant 0$. Note that the equivalent exchange terms, such as

$$\frac{1}{N_k}\sum_{i\mathbf{k},\,j\mathbf{k}'} \epsilon_{i\mathbf{k}} \epsilon_{j\mathbf{k}'} \overbrace{\hat{a}^\dagger_{j\mathbf{k}'} \hat{a}_{j\mathbf{k}'} \hat{a}^\dagger_{i\mathbf{k}} \hat{a}}\,_{i\mathbf{k}}, \tag{8}$$

tend to zero in the limit of an infinite k-point set. Before proceeding further, we will assume that the system is time-reversal symmetric; thus, if $\varphi_{i\mathbf{k}}(\mathbf{r})$ is an electronic orbital, then so is $\varphi^*_{i-\mathbf{k}}(\mathbf{r})$. This leads to the relationships

$$\Gamma^{\alpha\mathbf{q}}_{ij\mathbf{k}} = \Gamma^{\alpha\mathbf{q}}_{ji-\mathbf{k}-\mathbf{q}}, \quad \Gamma^{*\alpha\mathbf{q}}_{ij\mathbf{k}} = \Gamma^{\alpha-\mathbf{q}}_{ji\mathbf{k}+\mathbf{q}}, \quad \gamma^{\mathbf{k}}_{ij} = \gamma^{-\mathbf{k}}_{ji}. \tag{9}$$

The result of only keeping terms up to quadratic order is a Hamiltonian for which the fermions are decoupled from the bosons:

$$\hat{H} = \hat{H}_{\rm f} + \hat{H}_{\rm b}, \tag{10}$$

where

$$\hat{H}_{\rm f} = \sum_{ij,\mathbf{k}} A^{\mathbf{k}}_{ij} \hat{a}^\dagger_{i\mathbf{k}} \hat{a}_{j\mathbf{k}} + \tfrac{1}{2} B^{\mathbf{k}}_{ij} \hat{a}^\dagger_{i\mathbf{k}} \hat{a}^\dagger_{j-\mathbf{k}} - \tfrac{1}{2} B^{*\mathbf{k}}_{ij} \hat{a}_{i\mathbf{k}} \hat{a}_{j-\mathbf{k}} \tag{11}$$

and

$$\hat{H}_{\rm b} = \sum_{\alpha\alpha',\mathbf{q}} D^{\mathbf{q}}_{\alpha\alpha'} \hat{d}^\dagger_{\alpha\mathbf{q}} \hat{d}_{\alpha'\mathbf{q}} + \tfrac{1}{2} E^{\mathbf{q}}_{\alpha\alpha'} \hat{d}^\dagger_{\alpha\mathbf{q}} \hat{d}^\dagger_{\alpha'-\mathbf{q}} + \tfrac{1}{2} E^{*\mathbf{q}}_{\alpha\alpha'} \hat{d}_{\alpha\mathbf{q}} \hat{d}_{\alpha'-\mathbf{q}} + \sum_{\alpha} F^{\mathbf{q}=0}_{\alpha} (\hat{d}^\dagger_{\alpha\mathbf{q}=0} + \hat{d}_{\alpha\mathbf{q}=0}). \tag{12}$$

The matrices A and B are given explicitly as

$$A^{\mathbf{k}}_{ij} = \epsilon_{i\mathbf{k}}\delta_{ij} - \epsilon_{\rm F} + \sum_{\alpha} \Gamma^{\alpha\mathbf{q}=0}_{ij\mathbf{k}} \langle \hat{d}_{\alpha\mathbf{q}=0} + \hat{d}^\dagger_{\alpha\mathbf{q}=0} \rangle - \frac{2}{N_q\,\delta E_0} \sum_{i'j'} \sum_{\alpha\alpha'\mathbf{q}} \Gamma^{\alpha\mathbf{q}}_{i'j\mathbf{k}}\, \Gamma^{*\alpha'\mathbf{q}}_{j'i\mathbf{k}}\, \delta\gamma^{\mathbf{k}+\mathbf{q}}_{i'j'} [\langle \hat{d}_{\alpha\mathbf{q}} \hat{d}_{\alpha'-\mathbf{q}} \rangle + \langle \hat{d}^\dagger_{\alpha'\mathbf{q}} \hat{d}_{\alpha\mathbf{q}} \rangle + \langle \hat{d}^\dagger_{\alpha-\mathbf{q}} \hat{d}_{\alpha'-\mathbf{q}} \rangle + \langle \hat{d}^\dagger_{\alpha-\mathbf{q}} \hat{d}^\dagger_{\alpha'\mathbf{q}} \rangle], \tag{13}$$

$$B^{\mathbf{k}}_{ij} = -\frac{2}{N_q\,\delta E_0} \sum_{i'j'} \sum_{\alpha\alpha'\mathbf{q}} \Gamma^{\alpha\mathbf{q}}_{j'j\mathbf{k}}\, \Gamma^{*\alpha'\mathbf{q}}_{i'i\mathbf{k}} \langle \hat{a}_{i'\mathbf{k}+\mathbf{q}} \hat{a}_{j'-\mathbf{k}-\mathbf{q}} \rangle \times [\langle \hat{d}_{\alpha\mathbf{q}} \hat{d}_{\alpha'-\mathbf{q}} \rangle + \langle \hat{d}^\dagger_{\alpha'\mathbf{q}} \hat{d}_{\alpha\mathbf{q}} \rangle + \langle \hat{d}^\dagger_{\alpha-\mathbf{q}} \hat{d}_{\alpha'-\mathbf{q}} \rangle + \langle \hat{d}^\dagger_{\alpha-\mathbf{q}} \hat{d}^\dagger_{\alpha'\mathbf{q}} \rangle]. \tag{14}$$

The matrix D is related to E by

$$D^{\mathbf{q}}_{\alpha\alpha'} = \nu_{\alpha\mathbf{q}}\delta_{\alpha\alpha'} + E^{\mathbf{q}}_{\alpha\alpha'}, \tag{15}$$

with E arising from either the normal or anomalous electronic density matrices:

$$E^{\mathbf{q}}_{\alpha\alpha'} = -\frac{n_s}{N_k\,\delta E_0} \sum_{ij,i'j'\mathbf{k}} \Gamma^{*\alpha\mathbf{q}}_{ji\mathbf{k}}\, \Gamma^{\alpha'\mathbf{q}}_{i'j'\mathbf{k}}\, \delta\gamma^{\mathbf{k}+\mathbf{q}}_{i'j}\, \delta\gamma^{\mathbf{k}}_{ij'} \qquad \text{(normal)}, \tag{16}$$

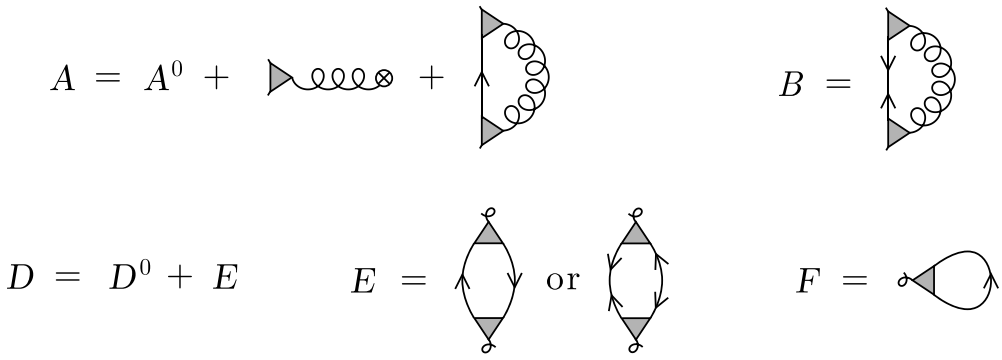

FIG. 1. Schematic representation of the matrices A, B, D, E, and F corresponding to the contractions in Eqs. (13)–(18), respectively. The components are the electron-phonon vertex $\Gamma =$; the change in electronic density matrix $\delta\gamma =$; the anomalous density matrix $\langle \hat{a}\,\hat{a}\rangle =$; the phonon densities $\langle \hat{d}\,\hat{d}\,\rangle + \langle \hat{d}^\dagger \hat{d}\rangle + \langle \hat{d}^\dagger \hat{d}\rangle + \langle \hat{d}^\dagger \hat{d}^\dagger\rangle =$, and $\langle \hat{d} + \hat{d}^\dagger\rangle =$.

$$E^{\mathbf{q}}_{\alpha\alpha'} = \frac{n_s}{N_k\,\delta E_0} \sum_{ij,i'j'\mathbf{k}} \Gamma^{*\alpha\mathbf{q}}_{ji\mathbf{k}}\,\Gamma^{\alpha'\mathbf{q}}_{i'j'\mathbf{k}}\,\langle \hat{a}_{j\mathbf{k}+\mathbf{q}}\hat{a}_{i'-\mathbf{k}-\mathbf{q}}\rangle\langle \hat{a}^\dagger_{i\mathbf{k}}\hat{a}^\dagger_{j'-\mathbf{k}}\rangle \quad \text{(anomalous)}. \tag{17}$$

Finally, the vector F is given by

$$F^{\mathbf{q}=0}_{\alpha} = \frac{n_s}{N_k} \sum_{ij\mathbf{k}} \Gamma^{\alpha\mathbf{q}=0}_{ij\mathbf{k}}\,\delta\gamma^{\mathbf{k}}_{ij}. \tag{18}$$

These terms are expressed diagramatically in Fig. 1, where instead of the propagators found in Feynman diagrams, there are electron and phonon density matrices connecting the vertices.

III. ALGEBRAIC FORM OF THE ELECTRON AND PHONON BOGOLIUBOV EQUATIONS

In the following, the k- and q-point dependencies of the fermionic and bosonic Hamiltonians are removed and we focus on their algebraic structure instead. All matrices are assumed to be finite in size.

A. Bogoliubov equation for electrons

The most general noninteracting fermionic Hamiltonian of interest here has the form

$$\hat{H}_{\mathrm{f}} = \sum_{i,j=1}^{n_{\mathrm{f}}} A_{ij}\hat{a}^\dagger_i\hat{a}_j + \tfrac{1}{2}B_{ij}\hat{a}^\dagger_i\hat{a}^\dagger_j - \tfrac{1}{2}B^*_{ij}\hat{a}_i\hat{a}_j, \tag{19}$$

where A is a Hermitian matrix; B is antisymmetric and corresponds to the matrix elements of the superconducting pairing potential $\Delta(\mathbf{r},\mathbf{r}')$. The sum runs to the number of fermionic basis vectors n_{f}. The matrix A includes a chemical potential term $A_{ij} \to A_{ij} + \mu\delta_{ij}$ which is used to fix the total electronic number to N_{e}. The Hermitian eigenvalue problem

$$\begin{pmatrix} A & B \\ B^\dagger & -A^* \end{pmatrix}\begin{pmatrix} \vec{U}_j \\ \vec{V}_j \end{pmatrix} = \varepsilon_j \begin{pmatrix} \vec{U}_j \\ \vec{V}_j \end{pmatrix} \tag{20}$$

yields $2n_{\mathrm{f}}$ solutions. However, if ε_j and $(\vec{U}_j, \vec{V}_j)$ are an eigenpair, then so are $-\varepsilon_j$ and $(\vec{V}^*_j, \vec{U}^*_j)$. Now we select n_{f} eigenpairs with each corresponding to either a positive or negative eigenvalue but with its conjugate partner not in the set. This choice will not affect the eventual ground state. Let U and V be the $n_{\mathrm{f}}\times n_{\mathrm{f}}$ matrices with these solutions arranged columnwise. Orthogonality of the vectors is then expressed as

$$\begin{pmatrix} U & V^* \\ V & U^* \end{pmatrix}^\dagger \begin{pmatrix} U & V^* \\ V & U^* \end{pmatrix} = I, \tag{21}$$

which implies $U^\dagger U + V^\dagger V = I$ and $U^\dagger V^* + V^\dagger U^* = 0$. Completeness further implies $UU^\dagger + V^*V^t = I$ and $UV^\dagger + V^*U^t = 0$. The Hamiltonian Eq. (19) can now be diagonalized with the aid of U and V via a Bogoliubov transformation [27]:,

$$\begin{aligned} \hat{\alpha}^\dagger_j &= \sum_{i=1}^{n_{\mathrm{f}}} U_{ij}\hat{a}^\dagger_i + V_{ij}\hat{a}_i, \\ \hat{\alpha}_j &= \sum_{i=1}^{n_{\mathrm{f}}} U^*_{ij}\hat{a}_i + V^*_{ij}\hat{a}^\dagger_i, \end{aligned} \tag{22}$$

in other words,

$$\hat{H}_{\mathrm{f}} = \sum_{i=1}^{n_{\mathrm{f}}} \varepsilon_i\hat{\alpha}^\dagger_i\hat{\alpha}_i + W_0, \tag{23}$$

where $W_0 = -\mathrm{tr}(V\varepsilon V^\dagger)$. The fermionic algebra is also preserved for $\hat{\alpha}$:

$$\{\hat{\alpha}_i, \hat{\alpha}^\dagger_j\} = \delta_{ij}, \quad \{\hat{\alpha}_i, \hat{\alpha}_j\} = 0, \quad \{\hat{\alpha}^\dagger_i, \hat{\alpha}^\dagger_j\} = 0. \tag{24}$$

1. Noninteracting ground state

Given A and B, the matrices U, V, and ε are fixed by the Bogoliubov Eq, (20). What remains is to construct from these the eigenstates of Eq. (19) in the Fock space. To do so, one first needs to find a normalized vacuum state which is annihilated by all the $\hat{\alpha}_j$. Here it is (denoted $|\bar{0}\rangle$ so as to distinguish it from the normal vacuum state $|0\rangle$),

$$|\bar{0}\rangle \equiv \prod_{j=1}^{n_{\mathrm{f}}} \hat{U}_j \prod_{k=1}^{n_{\mathrm{f}}} \hat{a}^\dagger_k|0\rangle + \prod_{j=1}^{n_{\mathrm{f}}} \hat{V}^\dagger_j|0\rangle, \tag{25}$$

where $\hat{U}_j \equiv \sum_i U^*_{ij}\hat{a}_i$ and $\hat{V}^\dagger_j \equiv \sum_i V^*_{ij}\hat{a}^\dagger_i$. It is readily verified that $\hat{\alpha}_j|\bar{0}\rangle = 0$ for all j; the vacuum has the correct normalization $\langle\bar{0}|\bar{0}\rangle = 1$; and the vacuum energy $\langle\bar{0}|H_{\mathrm{f}}|\bar{0}\rangle = W_0$. The noninteracting many-body ground state can be constructed in analogy with the usual fermionic situation. Let M be the

number of $\varepsilon_j < 0$, then the ground state

$$|\Phi_0\rangle = \prod_{j=1}^{M} \hat{\alpha}_j^\dagger |\bar{0}\rangle, \tag{26}$$

so

$$\hat{H}_\mathrm{f}|\Phi_0\rangle = E_0|\Phi_0\rangle, \tag{27}$$

where $E_0 = \sum_{j=1}^{M} \varepsilon_j + W_0$.

2. Normal and anomalous densities

To determine the densities, both normal and anomalous, one first has to find the expectation values of pairs of $\hat{a}$ and $\hat{a}^\dagger$. These, in turn, are linear combinations of expectation values of pairs of $\hat{\alpha}$ and $\hat{\alpha}^\dagger$. Using the anticommutation relations Eqs. (24) and remembering that $\hat{\alpha}|\bar{0}\rangle = 0$, we get

$$\begin{aligned}\langle\Phi_0|\hat{\alpha}_i^\dagger\hat{\alpha}_j|\Phi_0\rangle &= \begin{cases}\delta_{ij} & i,j \leqslant M\\ 0 & i,j > M\end{cases}\\ \langle\Phi_0|\hat{\alpha}_i\hat{\alpha}_j^\dagger|\Phi_0\rangle &= \begin{cases}0 & i,j \leqslant M\\ \delta_{ij} & i,j > M\end{cases}\end{aligned} \tag{28}$$

and

$$\langle\Phi_0|\hat{\alpha}_i^\dagger\hat{\alpha}_j^\dagger|\Phi_0\rangle = 0, \quad \langle\Phi_0|\hat{\alpha}_i\hat{\alpha}_j|\Phi_0\rangle = 0. \tag{29}$$

Equations (22), (28), and (29) give the normal and anomalous density matrices:

$$\langle\Phi_0|\hat{a}_i^\dagger\hat{a}_j|\Phi_0\rangle = \sum_{k=1}^{M} U_{ik}^* U_{jk} + \sum_{k=M+1}^{n_\mathrm{f}} V_{ik} V_{jk}^* \tag{30}$$

and

$$\langle\Phi_0|\hat{a}_i^\dagger\hat{a}_j^\dagger|\Phi_0\rangle = \sum_{k=1}^{M} U_{ik}^* V_{jk} + \sum_{k=M+1}^{n_\mathrm{f}} V_{ik} U_{jk}^*. \tag{31}$$

3. Time evolution

What remains is to determine how the fermionic state evolves with time in the time-dependent version of the method. The form of the ground-state equations dictates that of the time-dependent equations. Thus, if we assume that the matrices A and B are now functions of time, then the time-dependent generalization of Eq. (20) is

$$i\frac{\partial}{\partial t}\begin{pmatrix}\vec{U}_j\\ \vec{V}_j\end{pmatrix} = \begin{pmatrix}A(t) & B(t)\\ B^\dagger(t) & -A^*(t)\end{pmatrix}\begin{pmatrix}\vec{U}_j\\ \vec{V}_j\end{pmatrix}, \tag{32}$$

with the time-dependent state given by $|\Phi(t)\rangle = \prod_{i=1}^{M}\hat{\alpha}_i^\dagger(t)|\bar{0}\rangle$. It is easy to show that this state satisfies

$$\begin{aligned}&i\frac{\partial|\Phi(t)\rangle}{\partial t}\\ &= \left(\sum_{ij} A_{ij}(t)\hat{a}_i^\dagger\hat{a}_j + \tfrac{1}{2}B_{ij}(t)\hat{a}_i^\dagger\hat{a}_j^\dagger - \tfrac{1}{2}B_{ij}^*(t)\hat{a}_i\hat{a}_j\right)|\Phi(t)\rangle,\end{aligned} \tag{33}$$

with $|\Phi(t=0)\rangle = |\Phi_0\rangle$. Note that the number of occupied orbitals M remains constant with time. Here we have assumed that the system has evolved from its ground state.

B. Bogoliubov equation for phonons

The most general noninteracting bosonic Hamiltonian of relevance here has the form

$$\begin{aligned}\hat{H}_\mathrm{b} = &\sum_{ij} D_{ij}\hat{d}_i^\dagger\hat{d}_j + \tfrac{1}{2}E_{ij}\hat{d}_i^\dagger\hat{d}_j^\dagger + \tfrac{1}{2}E_{ij}^*\hat{d}_i\hat{d}_j\\ &+ \sum_i F_i\hat{d}_i^\dagger + F_i^*\hat{d}_i,\end{aligned} \tag{34}$$

where D is Hermitian and contains the kinetic energy operator; E is a complex symmetric matrix and F is a complex vector. Note that $\hat{H}_\mathrm{b}$ contains the anomalous terms $\hat{d}_i^\dagger\hat{d}_j^\dagger$ and $\hat{d}_i\hat{d}_j$. In analogy with the fermionic case, this Hamiltonian can be diagonalized,

$$\hat{H}_\mathrm{b} = \sum_{i=1}^{n_\mathrm{b}} \omega_i\hat{\gamma}_i^\dagger\hat{\gamma}_i + \Omega_0, \tag{35}$$

with the Bogoliubov-type transformation

$$\begin{aligned}\hat{\gamma}_j &= \sum_{i=1}^{n_\mathrm{b}} W_{ij}^*\hat{d}_i + X_{ij}^*\hat{d}_i^\dagger + y_j^*,\\ \hat{\gamma}_j^\dagger &= \sum_{i=1}^{n_\mathrm{b}} W_{ij}\hat{d}_i^\dagger + X_{ij}\hat{d}_i + y_j,\end{aligned} \tag{36}$$

where W and X are complex matrices and y is a complex vector. The index j runs from 1 to twice the number of bosonic modes. Requiring that $\hat{\gamma}$ and $\hat{\gamma}^\dagger$ obey bosonic algebra (the complex numbers y_j obviously commute with themselves and the operators, maintaining the algebra) yields

$$W^\dagger W - X^\dagger X = I, \tag{37}$$

$$W^\dagger X^* - X^\dagger W^* = 0. \tag{38}$$

After some manipulation, we arrive at the Bogoliubov equations for phonons:

$$\begin{pmatrix}D & -E\\ E^* & -D^*\end{pmatrix}\begin{pmatrix}\vec{W}_j\\ \vec{X}_j\end{pmatrix} = \omega_j\begin{pmatrix}\vec{W}_j\\ \vec{X}_j\end{pmatrix}. \tag{39}$$

The above equation cannot be reduced to a symmetric eigenvalue problem because the conditions Eqs. (37) and (38) correspond to the indefinite inner product $\eta = \mathrm{diag}(1,\ldots,1,-1,\ldots,-1)$. Such matrix Hamiltonians can still possess real eigenvalues [28–31] and this particular aspect is explored in Appendix A.

Once these equations are solved, the vector y is determined from

$$y = \omega^{-1}(W^t - X^t)F, \tag{40}$$

where $\omega = \mathrm{diag}(\omega_1,\ldots,\omega_{n_\mathrm{b}})$. The constant term in Eq. (35) given by

$$\Omega_0 = -\mathrm{tr}(X\omega X^\dagger) - y^\dagger\omega y. \tag{41}$$

1. Existence and nature of the vacuum state

We now show that the state which is annihilated by all the $\hat{\gamma}_i$ exists. Let

$$\hat{w}_j := \sum_{i=1}^{n_b} W_{ij}^* \hat{d}_i \quad \hat{x}_j^\dagger := \sum_{i=1}^{n_b} X_{ij}^* \hat{d}_i^\dagger, \tag{42}$$

then

$$[\hat{w}_j, \hat{x}_j^\dagger] = \sum_{i=1}^{n_b} W_{ij}^* X_{ij}^* =: \tau_j. \tag{43}$$

Now consider the eigenvalue equation:

$$(\hat{w}_j + \hat{x}_j^\dagger)|\bar{0}_j\rangle = -y_j^*|\bar{0}_j\rangle. \tag{44}$$

Using the ansatz

$$|\bar{0}_j\rangle = \sum_{n=0}^{\infty} \frac{\kappa_n^j}{n!}(\hat{x}_j^\dagger)^n|0\rangle, \tag{45}$$

we obtain a recurrence relation

$$\kappa_n^j = \left[-y_j^* \kappa_{n-1}^j - (n-1)\kappa_{n-2}^j\right]/\tau_j \tag{46}$$

with $y_j^* \kappa_0^j = -\kappa_1^j \tau_j$ and κ_0^j chosen so $\langle \bar{0}_j|\bar{0}_j\rangle = 1$. Note that if $\kappa_n^j = 1$ for all n then Eq. (45) is a coherent state. The vacuum state

$$|\bar{0}\rangle = \zeta \hat{S} \bigotimes_{j=1}^{n_b} |\bar{0}_j\rangle, \tag{47}$$

where ζ is a normalization constant and $\hat{S}$ is the symmetrizing operator, is annihilated by all $\hat{\gamma}_j$ and, because $\omega_j > 0$ for all j, is also the bosonic ground state, which is the lowest energy Fock space eigenstate of Eq. (34), as required.

2. Phononic observables and time evolution

To make the theory useful, observables which are products of the original $\hat{d}_i$ and $\hat{d}_i^\dagger$ operators have to be computed. After some straightforward algebra one finds that linear operators may be evaluated using

$$Y_i := \langle \bar{0}|\hat{d}_i|\bar{0}\rangle = \langle \bar{0}|\hat{d}_i^\dagger|\bar{0}\rangle^* = \sum_{j=1}^{n_b} X_{ij}^* y_j - W_{ij} y_j^*. \tag{48}$$

Observables which are quadratic are more complicated:

$$\begin{aligned} \langle \bar{0}|\hat{d}_i^\dagger \hat{d}_j|\bar{0}\rangle &= Y_i^* Y_j + (XX^\dagger)_{ij}, \quad \langle \bar{0}|\hat{d}_i \hat{d}_j^\dagger|\bar{0}\rangle = Y_i Y_j^* + (WW^\dagger)_{ij}, \\ \langle \bar{0}|\hat{d}_i^\dagger \hat{d}_j^\dagger|\bar{0}\rangle &= Y_i^* Y_j^* - (XW^\dagger)_{ij}, \quad \langle \bar{0}|\hat{d}_i \hat{d}_j|\bar{0}\rangle = Y_i Y_j - (WX^\dagger)_{ij}. \end{aligned} \tag{49}$$

The extension to the time-dependent case follows the same procedure as that for fermions, namely, that the matrices and vector D, E, and F in Eq. (34) become time-dependent as, consequently, do $\hat{\gamma}_i^\dagger$ and $|\bar{0}\rangle$ after solving the equation of motion:

$$i\frac{\partial}{\partial t}\begin{pmatrix} \vec{W}_j \\ \vec{X}_j \end{pmatrix} = \begin{pmatrix} D(t) & -E(t) \\ E^*(t) & -D^*(t) \end{pmatrix}\begin{pmatrix} \vec{W}_j \\ \vec{X}_j \end{pmatrix}. \tag{50}$$

This time evolution is not unitary but rather pseudounitary [32] and will not preserve ordinary vector lengths, in general, but will preserve the indefinite inner product. The vector y can be determined analogously from

$$i\frac{\partial y}{\partial t} = (W^t(t) - X^t(t))F(t). \tag{51}$$

Evolving Eqs. (50) and (51) in time is equivalent to doing the same for the second-quantized Hamiltonian and the Fock space state vector:

$$i\frac{\partial|\Phi(t)\rangle}{\partial t} = \left(\sum_{ij} D_{ij}(t)\hat{d}_i^\dagger \hat{d}_j + \tfrac{1}{2}E_{ij}(t)\hat{d}_i^\dagger \hat{d}_j^\dagger + \tfrac{1}{2}E_{ij}^*(t)\hat{d}_i \hat{d}_j + \sum_i F_i(t)\hat{d}_i^\dagger + F_i^*(t)\hat{d}_i\right)|\Phi(t)\rangle. \tag{52}$$

IV. IMPLEMENTATION FOR SOLIDS

Having established the electron and phonon Bogoliubov equations to be solved as well as expectation values of operator products, we can write the terms A, B, D, E, and F as functions of the quantities $(U_\mathbf{k}, V_\mathbf{k})$ and $(W_\mathbf{q}, X_\mathbf{q})$.

The normal electronic density matrix can be written

$$\gamma_{ij}^\mathbf{k} = \langle \hat{a}_{i\mathbf{k}}^\dagger \hat{a}_{j\mathbf{k}}\rangle = (V_\mathbf{k} V_\mathbf{k}^\dagger)_{ij}, \tag{53}$$

where we have used Eq. (30) and retained only the positive eigenvalues (as is our choice). All the terms in the H_f and H_b are determined in a similar manner:

$$\begin{aligned} A_{ij}^\mathbf{k} = {} & \epsilon_{i\mathbf{k}}\delta_{ij} - \epsilon_\mathrm{F} + 2\sum_\alpha \Gamma_{ij\,\mathbf{k}}^{\alpha\mathbf{q}=0}\,\mathrm{Re}\big(Y_\alpha^{\mathbf{q}=0}\big) \\ & - \frac{2}{N_q\,\delta E_0}\sum_{i'j'}\sum_{\alpha\alpha'\mathbf{q}} \Gamma_{i'j'\,\mathbf{k}}^{\alpha\mathbf{q}}\,\Gamma_{j'i\,\mathbf{k}}^{*\alpha'\mathbf{q}}\,\delta\gamma_{i'j'}^{\mathbf{k}+\mathbf{q}} \\ & \times [X_{-\mathbf{q}}X_{-\mathbf{q}}^\dagger - W_\mathbf{q}X_{-\mathbf{q}}^\dagger]_{\alpha\alpha'}, \end{aligned} \tag{54}$$

$$B^{\mathbf{k}}_{ij} = -\frac{2}{N_q\,\delta E_0}\sum_{i'j'}\sum_{\alpha\alpha'\mathbf{q}}\Gamma^{\alpha\mathbf{q}}_{j'j\mathbf{k}}\,\Gamma^{*\alpha'\mathbf{q}}_{i'i\mathbf{k}}\,(U_{\mathbf{k}+\mathbf{q}}V^{\dagger}_{-\mathbf{k}-\mathbf{q}})_{i'j'} \times [X_{-\mathbf{q}}X^{\dagger}_{-\mathbf{q}} - W_{\mathbf{q}}X^{\dagger}_{-\mathbf{q}}]_{\alpha\alpha'}, \tag{55}$$

$$E^{\mathbf{q}}_{\alpha\alpha'} = -\frac{n_s}{N_k\,\delta E_0}\sum_{ij,i'j'\mathbf{k}}\Gamma^{*\alpha\mathbf{q}}_{ji\mathbf{k}}\,\Gamma^{\alpha'\mathbf{q}}_{i'j'\mathbf{k}}\,\delta\gamma^{\mathbf{k}+\mathbf{q}}_{i'j}\,\delta\gamma^{\mathbf{k}}_{ij'} \quad \text{(normal)}, \tag{56}$$

$$E^{\mathbf{q}}_{\alpha\alpha'} = \frac{n_s}{N_k\,\delta E_0}\sum_{ij,i'j'\mathbf{k}}\Gamma^{*\alpha\mathbf{q}}_{ji\mathbf{k}}\,\Gamma^{\alpha'\mathbf{q}}_{i'j'\mathbf{k}}\,(U_{\mathbf{k}+\mathbf{q}}V^{\dagger}_{-\mathbf{k}-\mathbf{q}})_{ji'}(U_{\mathbf{k}}V^{\dagger}_{-\mathbf{k}})^{*}_{ij'} \quad \text{(anomalous)}, \tag{57}$$

$$D^{\mathbf{q}}_{\alpha\alpha'} = \nu_{\alpha\mathbf{q}}\delta_{\alpha\alpha'} + E^{\mathbf{q}}_{\alpha\alpha'}, \tag{58}$$

$$F^{\mathbf{q}=0}_{\alpha} = \frac{n_s}{N_k}\sum_{ij\mathbf{k}}\Gamma^{\alpha\mathbf{q}=0}_{ij\mathbf{k}}\delta\gamma^{\mathbf{k}}_{ij}. \tag{59}$$

Owing to time-reversal symmetry, the electron and phonon equations to be solved are

$$\begin{pmatrix} A_{\mathbf{k}} & B_{\mathbf{k}} \\ B^{\dagger}_{\mathbf{k}} & -A_{\mathbf{k}} \end{pmatrix}\begin{pmatrix} \vec{U}_{j\mathbf{k}} \\ \vec{V}_{j-\mathbf{k}} \end{pmatrix} = \varepsilon_{j\mathbf{k}}\begin{pmatrix} \vec{U}_{j\mathbf{k}} \\ \vec{V}_{j-\mathbf{k}} \end{pmatrix},$$
$$\begin{pmatrix} D_{\mathbf{q}} & -E_{\mathbf{q}} \\ E_{\mathbf{q}} & -D_{\mathbf{q}} \end{pmatrix}\begin{pmatrix} \vec{W}_{j\mathbf{q}} \\ \vec{X}_{j-\mathbf{q}} \end{pmatrix} = \omega_{j\mathbf{q}}\begin{pmatrix} \vec{W}_{j\mathbf{q}} \\ \vec{X}_{j-\mathbf{q}} \end{pmatrix}, \tag{60}$$

where $A_{\mathbf{k}}$, $D_{\mathbf{q}}$ and $E_{\mathbf{q}}$ are Hermitian and $B_{\mathbf{k}}$ is symmetric.

The above equations were implemented in the all-electron ELK code [33] which is a density functional theory (DFT) Kohn-Sham code and uses augmented plane waves as its basis. Phonon dispersions and the electron-phonon coupling matrix elements were determined using density functional perturbation theory (DFPT) [34]. The local density approximation (LDA) was used as the exchange-correlation functional throughout. The important issue of stability of the self-consistent procedure is addressed in Appendix B.

Anomalous correlation entropy

Before proceeding to the results, we first define a potentially useful quantity: the anomalous correlation entropy (ACE). Let $v_i \equiv |\vec{V}_i|^2$ be the norm squared of the V part of the vector $(\vec{U}_i, \vec{V}_i)$, and note that $0 \leqslant v_i \leqslant 1$. For a normal state (i.e., not superconducting) v_i is either 0 or 1. This suggests that we can define the fermionic ACE (FACE) as

$$\text{FACE} = -\sum_i v_i \ln(v_i) + (1 - v_i)\ln(1 - v_i), \tag{61}$$

which is a single, dimensionless quantity equal to zero for the normal state and greater than zero for the superconducting state. This is very similar to the correlation entropy of the one-reduced density matrix [35]. It is also possible to compute the FACE over a restricted sum of states, for example, those of a particular k point or simply for each individual state.

The bosonic ACE (BACE) is the analog for phonons. Here the X part of the vector $(\vec{W}_i, \vec{X}_i)$ is squared: $x_i \equiv |\vec{X}_i|^2$, which is positive and unbounded, and the formula for bosonic entropy is employed:

$$\text{BACE} = -\sum_i x_i \ln(x_i) - (1 + x_i)\ln(1 + x_i). \tag{62}$$

The BACE (and its q-point resolved variant) is useful for determining the strength of *virtual* phonon modes responsible for causing correlations in the electronic system.

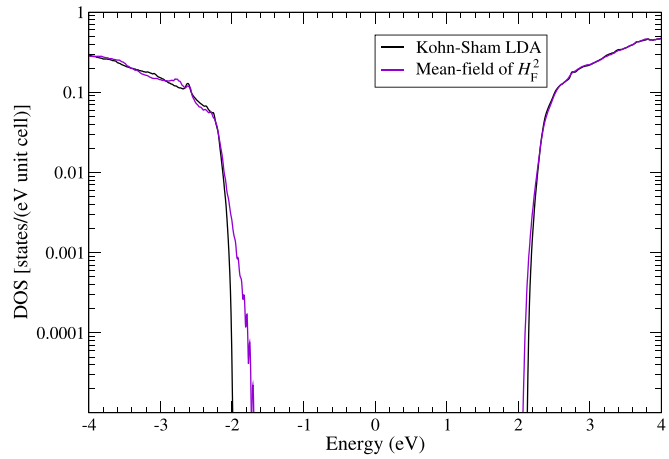

FIG. 2. Electronic density of states of diamond for both the conventional LDA Kohn-Sham system and the electron-phonon Bogoliubov equations derived from the mean field of $\hat{H}^2_{\text{F}}$.

V. RESULTS

A. Band-gap renormalization

1. Diamond

It has been known for some time that the band gap of diamond is significantly renormalized by the electron-phonon interaction [36–54]. We calculated the phonon dispersion and electron-phonon coupling matrix elements using DFPT with q-point and k-point grids both taken to be $16\times16\times16$. Calculations were performed using the experimentally determined lattice parameter. The electronic part electron-phonon system was solved in the basis of occupied orbitals plus 16 empty orbitals. Self-consistency was achieved in about 300 iterations. The density of states (DOS) is plotted in Fig. 2 for both the noninteracting (LDA) calculation and the electron-phonon calculation. Our calculated change in the fundamental (indirect) gap is −394 meV (from the Γ point to $(\frac{3}{8}, \frac{3}{8}, 0)$) and the change in the optical (direct) gap is −429 meV (Γ point). Table I lists band-gap renormalization energies from both experiment and theory. Previous theoretical results range from −462 meV to −321 meV for the fundamental gap and −670 meV to −409 meV for the optical gap. Experimental values range from −410 meV to −340 meV and −320 meV to −450 meV for the fundamental and optical gaps, respectively. This lack of consensus for the value both gap renormalization energies makes it difficult to judge the quality of our results. Both of the gaps determined using the current method lie within the range of both previous theory and experiment. Our indirect gap is closest to the experimental result of Monserrat *et al.* [40], which claims to be a more accurate extrapolation of the temperature-dependent

TABLE I. Band gap renormalization of diamond.

Reference	Fundamental gap renormalization (meV)	Optical gap renormalization (meV)
Experiment		
Logothetidis *et al.* [37]		−320, −450
Cardona [38]	−340	
Cardona [39]	−364, −370	
Monserrat *et al.* [40]	−410	
Theory		
Giustino *et al.* [41]		−615
Cannuccia and Marini [42]		−670
Monserrat and Needs [43]	−334	
Monserrat *et al.* [40]	−462	
Antonius *et al.* [44]		−404, −628
Poncé *et al.* [45]		−409
Lloyd-Williams and Monserrat [46]	−343	−430
Antonius *et al.* [47]		−320, −439
Poncé *et al.* [48]	−330	−416
Zacharias and Giustino [49]	−345	−450
Monserrat [50]	−344	
Monserrat [51]		∼ − 410, ∼ −642
Karsai *et al.* [52]	−320, −337	−326, −586
Miglio *et al.* [53]	−330	−416
Zhang *et al.* [54]	−437	
Current paper	−394	−429

thermal gap than previous estimates. Likewise, our optical gap is closest to the experimental value of Logothetidis *et al.* [37], determined from analyzing the second derivative of the dielectric function.

A significant observation is that most of the renormalization occurs at the valence band maximum with very little change to the conduction band DOS. This was also the conclusion reached by Engel *et al.* for the band gap renormalization of ice [55]. Precise resolution of this tail is critical for an accurate determination of the change in band gap. This, in turn, demands a sufficiently dense k-point set. The large variance among the theoretical results may be a consequence of some calculations being inadequately converged with respect to the number of k points.

Slices of the BACE across the Brillouin zone are plotted in Fig. 3 and are determined from Eq. (62), where the q point is fixed and the sum is only over the phonon branches. The values exhibit considerable variation, ranging from about 0.06 to 1.51. There are several hot spots throughout the zone where the virtual phonons which contribute to the renormalization of the electronic band gap are most prevalent. Those of highest intensity occur in the plane at $\mathbf{q} = \frac{1}{8}(1, 1, 1)$. We note that, like the k-point set, the strong variation of the BACE across the zone indicates that a large number of q points may be required to properly converge the renormalized gap.

2. Silicon

As a second example of band-gap renormalization, we applied the method to silicon. For this case, an $8\times8\times8$ q-point grid along with a shifted $16\times16\times16$ k-point grid was used. Our calculated gaps were quite similar to one another: −36 meV and [from the Γ point to $(0, \frac{9}{16}, \frac{9}{16})$] for the fundamental and −35 meV (Γ point) for the optical. These are in reasonable to good agreement with previous calculations and experiment (see Table II). The gap renormalization is over an order of magnitude smaller than that of diamond, indicating that the method works for a wide range of values.

The LDA and electron-phonon renormalized DOS is plotted in Fig. 4. Although the change in the gap is much smaller than that of diamond, the same characteristic that most of the effect arises from the highest occupied states is observed. The DOS of the conduction band is completely unchanged.

B. Superconductivity

Prediction of the superconducting state provides a stringent test for our method because of the very small energy scale of the superconducting gap compared to typical bandwidths. Accurate determination of the gap requires a large sampling of k points very close to the Fermi surface. In our calculations, a small shift was applied to the regular k-point grid, the effect of which is to reduce the number of equivalent points and thus distribute the eigenvalues more evenly around the Fermi energy. In addition, a small energy window was applied to the matrix elements of B in Eq. (55). All matrix elements corresponding to states with eigenvalues outside this window were set to zero. This is to ensure that only states very close to the Fermi energy can contribute to the anomalous density. The window was taken to be 0.001 Ha (∼27.2 meV) for all cases below. We found that the superconducting gap was fairly insensitive to this choice so long as there was a sufficient number of k points whose eigenvalues lay within this window. In both plots below, the points have been mirrored around zero to effectively increase the k-point sampling.

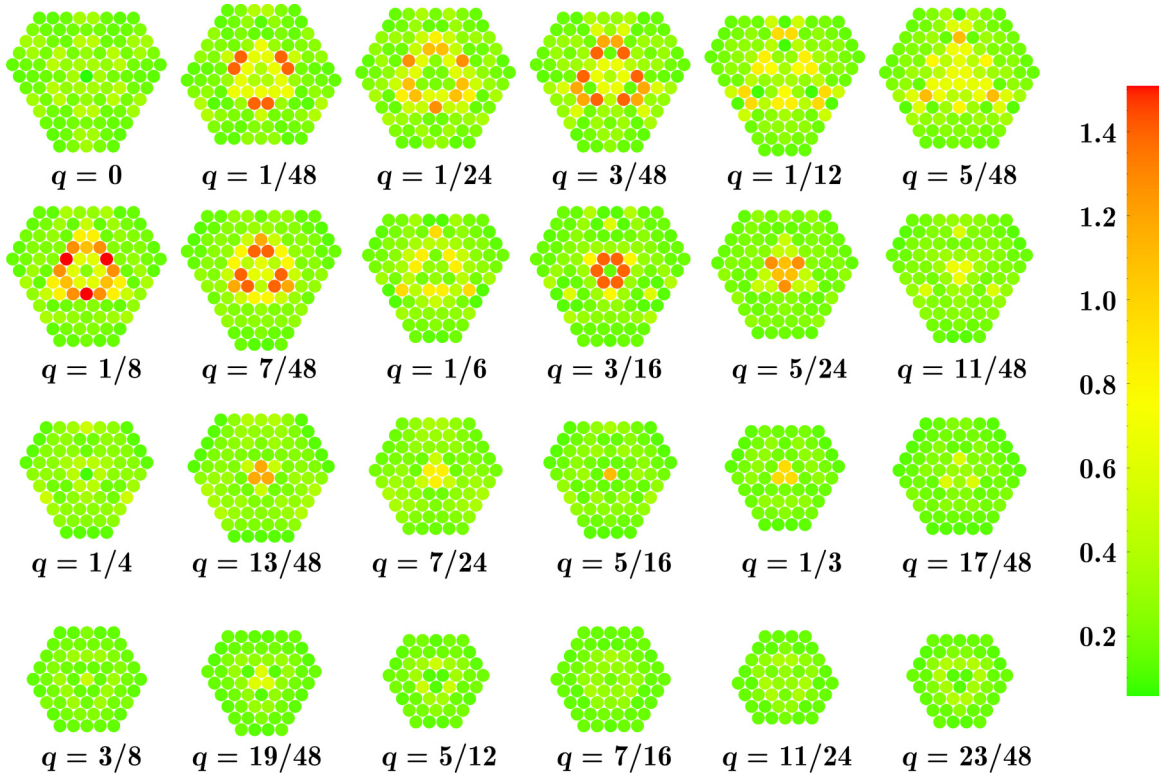

FIG. 3. Bosonic anomalous correlation entropy for diamond plotted across half the Brillouin zone. The vector at the center of each plane is given by $q(1, 1, 1)$ in reciprocal lattice coordinates. The value of the dimensionless BACE ranges from about 0.06 to 1.51.

It is important to mention that the anomalous Coulomb interaction is *not* included in these calculations, which generally results in superconducting gaps that are overestimated. We will compare our FACE to equivalent data calculated using the well-tested superconducting density functional theory (SCDFT) [58–62], where the effect of the Coulomb interaction has been deliberately omitted. The SCDFT code has the advantage of being able to upsample the k-point grid via interpolation to better resolve the superconducting gap. By convention, the superconducting gap should be measured from zero in the figures below. Note that the Fermi energy was continuously adjusted during the calculation to maintain the correct total charge.

1. Niobium

The phonon dispersion and electron-phonon matrix elements for bcc Nb were calculated on a 8×8×8 q-point set and a 40×40×40 k-point set shifted by $(\frac{1}{4}, \frac{1}{2}, \frac{5}{8})$ of the smallest

TABLE II. Band gap renormalization of silicon.

Reference	Fundamental gap renormalization (meV)	Optical gap renormalization (meV)
Experiment		
Lautenschlager [56]		−25
Cardona [38]	−50	
Pässler [57]	−72	
Cardona [39]	−60, −64	
Theory		
Monserrat *et al.* [43]	−60	
Poncé *et al.* [48]	−56	−42
Monserrat [50]	−58	
Monserrat [51]		−28
Zacharias and Giustino [49]	−57	−44
Karsai *et al.* [52]	−65	
Miglio *et al.* [53]	−56	−42
Zhang *et al.* [54]	−75	
Current paper	−36	−35

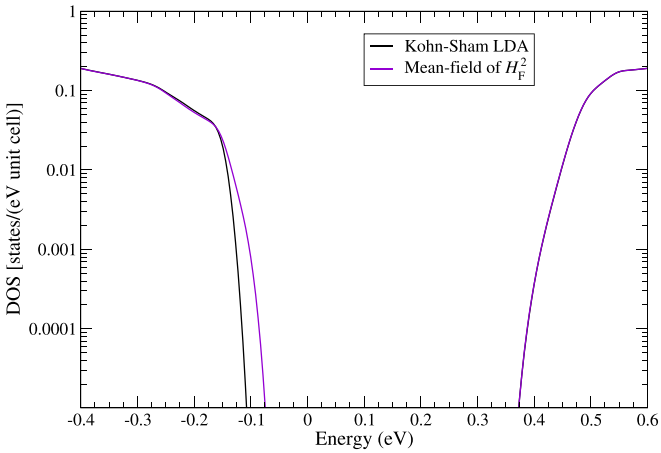

FIG. 4. Electronic density of states of silicon for both the conventional LDA Kohn-Sham system and the electron-phonon Bogoliubov equations derived from the mean-field of $\hat{H}_F^2$.

division. The total FACE converged in about 500 iterations. An energy-resolved histogram of the FACE for each state and k-point is presented in Fig. 5. This is compared to equivalent data calculated using SCDFT. One can see immediately that the FACE is nonzero in a region around the Fermi energy and that there is also a gap present. Owing to the scattered nature

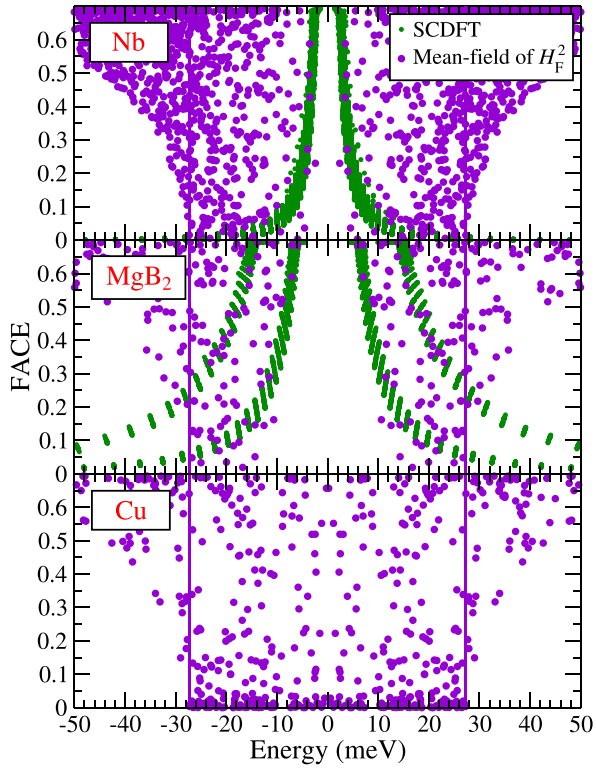

FIG. 5. State and k-point resolved FACE histogram of niobium, MgB_2, and copper calculated with SCDFT and the electron-phonon Bogoliubov equations derived from the mean-field of $\hat{H}_F^2$. The vertical lines indicate the energy cutoff used when evaluating the matrix B in Eq. (55). In both plots, the points have been mirrored around zero to effectively increase the k-point sampling.

of the points in the histogram, the precise value of the gap itself is difficult to ascertain. The minimum gap based on a single point is 2.4 meV. SCDFT (without Coulomb) gives a value of 2.5 meV, although this does not correspond to the single point with smallest gap but rather the midpoint of the main cluster of points taken at maximum FACE value. There is good agreement between our mean-field theory and SCDFT for the inner boundary of the FACE over the complete range of energies. One of the more recent experiments puts the value of the Nb superconducting gap at 1.49 meV [63]. The SCDFT gap with the Coulomb interaction included yields a gap of between 1.54 and 1.79 meV [60], indicating the magnitude of this effect. Including the anomalous Coulomb interaction in our calculations should also reduce our gap to about this value.

2. MgB_2

The superconducting state of MgB_2 is much more difficult to converge with respect to the number of k points than Nb. This is because its Fermi surface contains two-dimensional cylinderlike structures [64] which require particularly careful sampling. We used a k-point grid of $36\times36\times24$ shifted by $(\frac{1}{4}, \frac{1}{2}, \frac{5}{8})$ of the smallest division. The q-point set was taken to be $12\times12\times6$. The DFPT calculation generated about 140 GB of electron-phonon coupling data, putting it at the limit of our computational resources. This limitation and the form of the Fermi surface meant the resolution of the gap was not as good as for Nb. Convergence of the total FACE was achieved in about 500 iterations and took over 700 CPU hours, which was the most of all our calculations.

The state and k-point resolved FACE energy histogram can be see in Fig. 5. Distinct from the case of Nb is the appearance of two superconducting gaps in the plot. This is because the MgB_2 Fermi surface arises from two sets of bands with σ and π character [64]. Despite the noise, we estimate the π band gap from the single FACE point closest to zero, as 5.9 meV. This agrees well with the SCDFT value of 6.5 meV. On the whole, the inner boundary of the π band FACE is in good agreement with that of SCDFT.

It is nearly impossible to reliably extract a value for the second gap because of the sparsity of sampled points. SCDFT yields a value of about 15 meV. Nevertheless, an inner boundary of the σ gap can be discerned and follows that obtained from SCDFT. Better resolution of the σ gap of MgB_2 clearly requires a much denser k-point grid; this could be accomplished by an upsampling of the grid, as done in the SCDFT code.

3. *Copper*

Copper does not exhibit superconducting properties even at vanishingly small temperatures but rather possesses a residual resistance. Our method should therefore predict a superconducting gap of zero for this metal. The phonon dispersion and matrix elements were calculated for fcc Cu using a $8\times8\times8$ q-point grid and a $40\times40\times40$ k-point grid. The total FACE was considerably smaller than that for Nb and MgB_2, and converged in about 800 iterations. The state and k-point resolved FACE energy histogram can be seen in Fig. 5 and the absence of a gap is immediately apparent. This is an important test for

the Bogoliubov equations because it demonstrates that they did not produce a false positive for superconductivity, i.e., they correctly predict that fcc Cu should *not* be a superconductor even at a zero temperature.

VI. SUMMARY

We have defined noninteracting Hamiltonians for fermions and bosons which are coupled only via their respective density matrices. Both are solved using Bogoliubov equations: the fermionic are Hermitian and the bosonic are Hermitian only with respect to an indefinite metric. Sufficient conditions which guarantee real eigenvalues for the bosonic system were found. Explicit forms of the potential matrix elements A, B, D, E, and F which constitute the equations were found using mean-field potentials derived from Wick's theorem applied to the square of the Fröhlich Hamiltonian. Electron and phonon density matrices were determined by solving the equations together and self-consistently. We found that this approach correctly reproduced the renormalization of the band gaps in diamond and silicon. The superconducting gaps of bcc Nb and MgB_2 were shown to reproduce those of SCDFT, and fcc Cu was found to be nonsuperconducting, in accordance with experiment.

Based on these results, we are confident that this is a practical method for parameter-free simulations of the time evolution of the superconducting state. Furthermore, these equations and the application of Wick's theorem to the square of a Hamiltonian could be used for other theories with bosonic fields. One such example is quantum electrodynamics (QED), for which the method may be useful for studying strong field dynamics which include pair creation effects, or for cavity QED with discrete photon modes.

ACKNOWLEDGMENTS

We would like to thank James Annett for pointing out the similarity of our bosonic analysis to that in Ref. [65] and also thank Antonio Sanna for useful discussions and providing the SCDFT data. Calculations were performed on the Raven supercomputer at the Max Planck Computing and Data Facility. S.S. and J.K.D. would like to thank TRR227 (Project No. A04) for funding. E.K.U.G. would like to acknowledge the European Research Council (ERC) under the European Union's Horizon 2020 research and innovation program (Grant Agreement No. ERC-2017-AdG-788890).

APPENDIX A: MATHEMATICAL PROPERTIES OF THE BOSONIC BOGOLIUBOV EQUATIONS

In this Appendix, we prove that under certain conditions the matrix Eq. (39) always possesses n_b solutions which satisfy Eqs. (37) and (38). This requires the observation that if the vector $v \equiv (w, x)$ with eigenvalue ω is a solution to Eq. (39), then so is $\bar{v} \equiv (x, w)$ with eigenvalue $-\omega$. To simplify the arguments, we consider only the special case where the matrices D and E are real symmetric and the vector F is also real. In this case, the bosonic Hamiltonian can be written as

$$\hat{H}_\mathrm{b} = \sum_{ij} D_{ij}\hat{d}_i^\dagger \hat{d}_j + \tfrac{1}{2}E_{ij}(\hat{d}_i^\dagger \hat{d}_j^\dagger + \hat{d}_i\hat{d}_j) + \sum_i F_i(\hat{d}_i^\dagger + \hat{d}_i). \tag{A1}$$

Theorem 1. Let

$$H = \begin{pmatrix} D & -E \\ E & -D \end{pmatrix},$$

where D and E are real symmetric $n_\mathrm{b}\times n_\mathrm{b}$ matrices. Suppose H has only real, nondegenerate eigenvalues and every eigenvector v satisfies $v^t\eta v \neq 0$. Then

(1) The eigenvectors of H may be chosen real.

(2) The eigenvalue Eq. (39) has exactly n_b solutions which satisfy the conditions Eqs. (37) and (38).

Proof. The proof that the eigenvectors may be chosen real is straightforward, so we now prove the second statement. Let v_1 and v_2 be two real eigenvectors of H with corresponding real eigenvalues ω_1 and ω_2. Now $Hv_1 = \omega_1 v_1 \Rightarrow \eta H v_1 = \omega_1 \eta v_1$ and because ηH is symmetric we have $v_1^t \eta H = \omega_1 v_1^t \eta$ and thus $v_1^t \eta H v_2 = \omega_1 v_1^t \eta v_2$. We also have that $Hv_2 = \omega_2 v_2$ and so $v_1^t \eta H v_2 = \omega_2 v_1^t \eta v_2$. Subtracting and using the fact that $\omega_1 \neq \omega_2$ yields $v_1^t \eta v_2 = 0$. This is equivalent to the off-diagonal part of condition Eq. (37). Consider an eigenvector $v = (w, x)$ of H. Now $v^t\eta v \neq 0$, thus if $v^t\eta v < 0$ then choose the other eigenvector $\bar{v}$ for which $\bar{v}^t\eta\bar{v} > 0$. Such an eigenvector can be rescaled arbitrarily to ensure $v^t\eta v = 1$. This corresponds to the diagonal part of Eq. (37) but is valid for only half of the total number of eigenvectors since rescaling cannot change the sign of $v^t\eta v$. These remaining vectors are discarded. Condition Eq. (38) is trivially satisfied for the diagonal. For any two vectors v_i and v_j, suppose $v_j \neq \bar{v}_i$ then $\bar{v}_j = v_k$ for some other k. The off-diagonal part of condition Eq. (37) is satisfied for all vectors, thus $v_i^t\eta v_k = v_i^t\eta\bar{v}_j = 0$. If $v_j = \bar{v}_i$, then one of these vectors will have been discarded.

The theorem is easily extended to the case where H has degenerate eigenvalues. There is no guarantee that the eigenvalues of H are real since the matrix is not Hermitian. We therefore need additional restrictions on the matrices D and E to ensure this; the following conditions are sufficient but not necessary. We use the notation $P \succ 0$ to mean that the symmetric matrix P is positive definite, and that $P \succ Q$ implies $P - Q \succ 0$.

Theorem 2. Let $D \succ 0$, and suppose that E is a symmetric matrix. If any of the following are true then H has real eigenvalues:

(1) $D \succ ED^{-1}E$.

(2) The largest eigenvalue of $(ED^{-1})^2$ is less than 1.

(3) $z^\dagger Dz > |z^\dagger Ez|$ for all $z \in \mathbb{C}^{n_\mathrm{b}}$.

(4) $E \succ 0$ and $D \succ E$.

(5) $E \succ 0$ and $D^p \succ E^p$, where $p \geqslant 1$.

(6) $D^2 \succ E^2$.

Furthermore, if all eigenvalues are nonzero, then all eigenvectors satisfy $v^t\eta v \neq 0$.

Proof. Let ω and v be an eigenvalue and eigenvector of H. The matrix

$$\eta H = \begin{pmatrix} D & -E \\ -E & D \end{pmatrix}$$

is symmetric, therefore both sides of $v^\dagger \eta H v = \omega v^\dagger \eta v$ are real. The only requirement for ω to be real is that $v^\dagger \eta H v$ be nonzero, which is ensured so long as $\eta H \succ 0$. This follows from either of the conditions (i) or (ii) (see, for example, Ref. [66]). Condition (iii) follows from Theorem 2.1 in Ref. [67] and (iv) follows immediately. The Löwner-Heinz theorem [68] reduces condition (v) to (iv). Finally, suppose $D^2 \succ E^2$, where E may not be positive definite. E is symmetric, therefore $E^2 \succ 0$, which means that there exists a symmetric matrix $e \succ 0$ such that $e^2 = E^2$. The Löwner-Heinz theorem implies that $D \succ e$, therefore $z^\dagger D z > z^\dagger e z$ for all complex vectors $z \in \mathbb{C}^{n_b}$. E and e can be simultaneously diagonalized and for each eigenvalue λ of E there is a corresponding positive eigenvalue $|\lambda|$ of e. In this eigenvector basis, it is easy to see that $z^\dagger e z \geqslant |z^\dagger E z|$ for all z, which in turn gives condition (iii), thereby proving (vi). In fact, all of the above conditions imply [67] that $\eta H \succ 0$. Thus, if all eigenvalues $\omega \neq 0$, then $v^t \eta v \neq 0$.

Corollary 2.1. Let $D_0 \succ 0$ and $E \succeq 0$ (positive semidefinite), then $D = D_0 + E$ yields real eigenvalues for H.

Theorem 3. Let D be an arbitrary real symmetric matrix and let f be a real function such that $|f(x)| < |x|$ for all $x \in \mathbb{R}$, then by setting $E = f(D)$ (in the usual function of matrices sense [69]), H has real eigenvalues and every eigenvector v satisfies $v^t \eta v \neq 0$.

Proof. We first note that

$$H^2 = \begin{pmatrix} D^2 - E^2 & [E, D] \\ [E, D] & D^2 - E^2 \end{pmatrix}.$$

It is obvious for any $E = f(D)$ that $[E, D] = 0$ and $D^2 \succ E^2$. Therefore, all the eigenvalues of H^2 are real and positive. We conclude that the eigenvalues of H are real and nonzero, thus $v^t \eta v \neq 0$ follows from Theorem 2.

Theorem 4. Let D be a real symmetric matrix which has no zero eigenvalues and which commutes with all the matrices in a group representation $S = \{S_i\}$. Further suppose that any degenerate eigenvalues of D correspond only to irreducible representations of S (i.e., there are no accidental degeneracies). If E is a real symmetric matrix which also commutes with all the matrices in S, then there exists a $\xi > 0$ such that if $E \to \xi E$ then $H(\xi)$ has real eigenvalues.

Proof. From the properties of the determinant applied to blocked matrices, the eigenvalues of H^2 are also the eigenvalues of $Q := D^2 - E^2 + [E, D]$. Since $[D, S_i] = [E, S_i] = 0$ for all i, then D^2, E^2, $[E, D]$ and thus $Q(\xi)$ also commute with S_i. Schur's lemma applies equally well to non-Hermitian matrices, therefore the degeneracies of $Q(\xi)$ are not lost as ξ increases. We also note that the roots of a polynomial depend continuously on its coefficients and hence the eigenvalues of $Q(\xi)$ depend continuously on ξ. From the conjugate root theorem, if $Q(\xi)$ has a complex eigenvalue then it must also have its complex conjugate as an eigenvalue. For sufficiently small $\xi > 0$, the eigenvalues of D^2 cannot become complex because this would require lifting of a degeneracy. Also, because of continuity and because D^2 has strictly positive eigenvalues, a sufficiently small $\xi > 0$ will keep them positive. Hence the eigenvalues of $H(\xi)$ are real.

APPENDIX B: STABILITY OF THE BOGOLIUBOV EQUATIONS

We discovered from our initial implementation of the Bogoliubov equations that the self-consistent procedure was highly unstable and difficult or impossible to converge. The reasons for this are twofold: First, in each of the Eqs. (54)–(58), there is a division by δE_0. If this number becomes very small, then the terms in the Hamiltonian become large. In the next iteration, δE_0 is then large and the terms are small. Consequently, δE_0 becomes small again. This oscillatory behavior can be tamed by mixing the input and output density matrices with a small mixing parameter. A second and more severe source of instability is the indefinite metric required for solving the bosonic Bogoliubov Eq. (39). Typically, the right eigenvectors of a non-Hermitian matrix returned by a numerical linear algebra package such as LAPACK [70] are normalized to 1 using the regular Euclidean norm. However, an eigenvector which is a solution to Eq. (39) should have pseudonorm $|\vec{W}_i|^2 - |\vec{X}_i|^2 = 1$. If β_i is the pseudonorm of the vector $(\vec{W}_i, \vec{X}_i)$ with Euclidean norm 1, then we have to scale it by $1/\sqrt{\beta_i}$ to normalize it correctly. This is an obvious source of instability because β_i can be arbitrarily close to zero. Such instability can be cured by making the observation that the effect of electron-phonon coupling on the phonon system is usually so small that $\beta_i \simeq |\vec{W}_i|^2 \simeq 1$. Thus, we instead scale the vector by $[1 - (1 - \beta_i)^p]/\sqrt{\beta_i}$, where p is usually taken to be 2, although we find that the converged results are independent of this choice. This scaling approaches the original for β_i close to 1 but is equal to 0 for $\beta_i \to 0$. The combination of the modified scaling and slow mixing allow the calculations to achieve self-consistency.

[1] M. Born and R. Oppenheimer, Ann. Phys. **389**, 457 (1927).

[2] M. Born and K. Huang, *Dynamical Theory of Crystal Lattices* (Oxford University Press, London, 1956).

[3] W. Kutzelnigg, Mol. Phys. **90**, 909 (1997).

[4] W. Kutzelnigg, Mol. Phys. **105**, 2627 (2007).

[5] J. Bardeen, L. N. Cooper, and J. R. Schrieffer, Phys. Rev. **108**, 1175 (1957).

[6] D. Polli, P. Altoè, O. Weingart, K. M. Spillane, C. Manzoni, D. Brida, G. Tomasello, G. Orlandi, P. Kukura, R. A. Mathies, M. Garavelli, and G. Cerullo, Nature (London) **467**, 440 (2010).

[7] A. H. Zewail, J. Phys. Chem. A **104**, 5660 (2000).

[8] I. Schapiro, P. El-Khoury, and M. Olivucci, in *Handbook of Computational Chemistry* (Springer Netherlands, Amsterdam, 2012), p. 1359.

[9] G. D. Scholes, G. R. Fleming, A. Olaya-Castro, and R. van Grondelle, Nat. Chem. **3**, 763 (2011).

[10] M. Cardona and M. L. W. Thewalt, Rev. Mod. Phys. **77**, 1173 (2005).

[11] R. Requist, C. R. Proetto, and E. K. U. Gross, Phys. Rev. B **99**, 165136 (2019).

[12] W. S. Fann, R. Storz, H. W. K. Tom, and J. Bokor, Phys. Rev. B **46**, 13592 (1992).

[13] J. K. Dewhurst, P. Elliott, S. Shallcross, E. K. U. Gross, and S. Sharma, Nano Lett. **18**, 1842 (2018).

[14] C. A. Rozzi, S. A. Falke, N. Spallanzani, A. Rubio, E. Molinari, D. Brida, M. Maiuri, G. Cerullo, H. Schramm, J. Christoffers, and C. Lienau, Nat. Commun. **4**, 1602 (2013).

[15] S. M. Falke, C. A. Rozzi, D. Brida, M. Maiuri, M. Amato, E. Sommer, A. De Sio, A. Rubio, G. Cerullo, E. Molinari, and C. Lienau, Science **344**, 1001 (2014).

[16] T. R. Nelson, A. J. White, J. A. Bjorgaard, A. E. Sifain, Y. Zhang, B. Nebgen, S. Fernandez-Alberti, D. Mozyrsky, A. E. Roitberg, and S. Tretiak, Chem. Rev. **120**, 2215 (2020).

[17] W. Kohn, Phys. Rev. Lett. **2**, 393 (1959).

[18] R. J. McQueeney, Y. Petrov, T. Egami, M. Yethiraj, G. Shirane, and Y. Endoh, Phys. Rev. Lett. **82**, 628 (1999).

[19] W. Kohn and L. J. Sham, Phys. Rev. **140**, A1133 (1965).

[20] H. Fröhlich, Adv. Phys. **3**, 325 (1954).

[21] D. Karlsson, R. van Leeuwen, Y. Pavlyukh, E. Perfetto, and G. Stefanucci, Phys. Rev. Lett. **127**, 036402 (2021).

[22] A. Cavalleri, Contemp. Phys. **59**, 31 (2018).

[23] S. J. Zhang, Z. X. Wang, H. Xiang, X. Yao, Q. M. Liu, L. Y. Shi, T. Lin, T. Dong, D. Wu, and N. L. Wang, Phys. Rev. X **10**, 011056 (2020).

[24] M. Buzzi, D. Nicoletti, M. Fechner, N. Tancogne-Dejean, M. A. Sentef, A. Georges, T. Biesner, E. Uykur, M. Dressel, A. Henderson, T. Siegrist, J. A. Schlueter, K. Miyagawa, K. Kanoda, M.-S. Nam, A. Ardavan, J. Coulthard, J. Tindall, F. Schlawin, D. Jaksch *et al.*, Phys. Rev. X **10**, 031028 (2020).

[25] M. Budden, T. Gebert, M. Buzzi, G. Jotzu, E. Wang, T. Matsuyama, G. Meier, Y. Laplace, D. Pontiroli, M. Riccò, F. Schlawin, D. Jaksch, and A. Cavalleri, Nat. Phys. **17**, 611 (2021).

[26] F. Scheck, *Quantum Physics* (Springer, Berlin, 2007), pp. 317–320.

[27] N. N. Bogoliubov, J. Phys. (Moscow) **11**, 23 (1947).

[28] E. C. G. Sudarshan, Phys. Rev. **123**, 2183 (1961).

[29] A. Mostafazadeh, J. Math. Phys. **43**, 205 (2002).

[30] C. F. M. Faria and A. Fring, Laser Phys. **17**, 424 (2007).

[31] L. Zhang, J. Ren, J. S. Wang, and B. Li, J. Phys.: Condens. Matter **23**, 305402 (2011).

[32] A. Mostafazadeh, J. Math. Phys. **45**, 932 (2004).

[33] The Elk Code, http://elk.sourceforge.net/.

[34] S. Baroni, P. Giannozzi, and A. Testa, Phys. Rev. Lett. **58**, 1861 (1987).

[35] D. M. Collins, Z. Naturforsch. A **48**, 68 (1993).

[36] S. Zollner, M. Cardona, and S. Gopalan, Phys. Rev. B **45**, 3376 (1992).

[37] S. Logothetidis, J. Petalas, H. M. Polatoglou, and D. Fuchs, Phys. Rev. B **46**, 4483 (1992).

[38] M. Cardona, Physica Status Solidi (a) **188**, 1209 (2001).

[39] M. Cardona, Solid State Commun. **133**, 3 (2005).

[40] B. Monserrat, G. J. Conduit, and R. J. Needs, Phys. Rev. B **90**, 184302 (2014).

[41] F. Giustino, S. G. Louie, and M. L. Cohen, Phys. Rev. Lett. **105**, 265501 (2010).

[42] E. Cannuccia and A. Marini, Eur. Phys. J. B **85**, 320 (2012).

[43] B. Monserrat and R. J. Needs, Phys. Rev. B **89**, 214304 (2014).

[44] G. Antonius, S. Poncé, P. Boulanger, M. Côté, and X. Gonze, Phys. Rev. Lett. **112**, 215501 (2014).

[45] S. Poncé, G. Antonius, P. Boulanger, E. Cannuccia, A. Marini, M. Côté, and X. Gonze, Comput. Mater. Sci. **83**, 341 (2014).

[46] J. H. Lloyd-Williams and B. Monserrat, Phys. Rev. B **92**, 184301 (2015).

[47] G. Antonius, S. Poncé, E. Lantagne-Hurtubise, G. Auclair, X. Gonze, and M. Côté, Phys. Rev. B **92**, 085137 (2015).

[48] S. Poncé, Y. Gillet, J. Laflamme Janssen, A. Marini, M. Verstraete, and X. Gonze, J. Chem. Phys. **143**, 102813 (2015).

[49] M. Zacharias and F. Giustino, Phys. Rev. B **94**, 075125 (2016).

[50] B. Monserrat, Phys. Rev. B **93**, 014302 (2016).

[51] B. Monserrat, Phys. Rev. B **93**, 100301(R) (2016).

[52] F. Karsai, M. Engel, E. Flage-Larsen, and G. Kresse, New J. Phys. **20**, 123008 (2018).

[53] A. Miglio, V. Brousseau-Couture, E. Godbout, G. Antonius, Y.-H. Chan, S. G. Louie, M. Côté, M. Giantomassi, and X. Gonze, npj Comput. Mater. **6**, 167 (2020).

[54] Y. Zhang, Z. Wang, J. Xi, and J. Yang, J. Phys.: Condens. Matter **32**, 475503 (2020).

[55] E. A. Engel, B. Monserrat, and R. J. Needs, J. Chem. Phys. **143**, 244708 (2015).

[56] P. Lautenschlager, M. Garriga, L. Vina, and M. Cardona, Phys. Rev. B **36**, 4821 (1987).

[57] R. Pässler, Phys. Rev. B **66**, 085201 (2002).

[58] L. N. Oliveira, E. K. U. Gross, and W. Kohn, Phys. Rev. Lett. **60**, 2430 (1988).

[59] M. Lüders, M. A. L. Marques, N. N. Lathiotakis, A. Floris, G. Profeta, L. Fast, A. Continenza, S. Massidda, and E. K. U. Gross, Phys. Rev. B **72**, 024545 (2005).

[60] M. A. L. Marques, M. Lüders, N. N. Lathiotakis, G. Profeta, A. Floris, L. Fast, A. Continenza, E. K. U. Gross, and S. Massidda, Phys. Rev. B **72**, 024546 (2005).

[61] A. Sanna, C. Pellegrini, and E. K. U. Gross, Phys. Rev. Lett. **125**, 057001 (2020).

[62] A. Sanna (Private Communication).

[63] A. V. Pronin, M. Dressel, A. Pimenov, A. Loidl, I. V. Roshchin, and L. H. Greene, Phys. Rev. B **57**, 14416 (1998).

[64] I. I. Mazin and V. P. Antropov, Physica C **385**, 49 (2003).

[65] J. H. P. Colpa, Physica A **93**, 327 (1978).

[66] R. A. Horn and C. R. Johnson, *Matrix Analysis* (Cambridge University Press, Cambridge, 1990) Chap. 7, p. 473.

[67] C. H. Fitzgerald and R. A. Horn, J. London Math. Soc. **s2-15**, 419 (1977).

[68] X. Zhan, *Matrix Inequalities* (Springer-Verlag, Berlin, 2002), Chap. 1, p. 2.

[69] R. F. Rinehart, Amer. Math. Monthly **62**, 395 (1955).

[70] E. Anderson, Z. Bai, C. Bischof, S. Blackford, J. Demmel, J. Dongarra, J. Du Croz, A. Greenbaum, S. Hammarling, A. McKenney, and D. Sorensen, *LAPACK Users' Guide*, 3rd ed. (Society for Industrial and Applied Mathematics, Philadelphia, PA, 1999).